Colias: An Autonomous Micro Robot for Swarm Robotic Applications

4 authors:

Farshad Arvin
The University of Manchester
143 PUBLICATIONS   3,071 CITATIONS

SEE PROFILE

John Christopher Murray
University of Sunderland
50 PUBLICATIONS   585 CITATIONS

SEE PROFILE

Chun Zhang
Xi'an Jiaotong University
285 PUBLICATIONS   2,342 CITATIONS

SEE PROFILE

Shigang Yue
University of Leicester
272 PUBLICATIONS   4,189 CITATIONS

SEE PROFILE

Colias: An Autonomous Micro Robot for Swarm Robotic Applications

Regular Paper

Farshad Arvin[1], John Murray[1], Chun Zhang[2] and Shigang Yue[1,*]

1 School of Computer Science, University of Lincoln, Lincoln, UK
2 Institute of Microelectronics, Tsinghua University, Beijing, China
* Corresponding author E-mail: syue@lincoln.ac.uk

Abstract Robotic swarms that take inspiration from nature are becoming a fascinating topic for multi-robot researchers. The aim is to control a large number of simple robots in order to solve common complex tasks. Due to the hardware complexities and cost of robot platforms, current research in swarm robotics is mostly performed by simulation software. The simulation of large numbers of these robots in robotic swarm applications is extremely complex and often inaccurate due to the poor modelling of external conditions. In this paper, we present the design of a low-cost, open-platform, autonomous micro-robot (Colias) for robotic swarm applications. Colias employs a circular platform with a diameter of 4 cm. It has a maximum speed of 35 cm/s which enables it to be used in swarm scenarios very quickly over large arenas. Long-range infrared modules with an adjustable output power allow the robot to communicate with its direct neighbours at a range of 0.5 cm to 2 m. Colias has been designed as a complete platform with supporting software development tools for robotics education and research. It has been tested in both individual and swarm scenarios, and the observed results demonstrate its feasibility for use as a micro-sized mobile robot and as a low-cost platform for robot swarm applications.

Keywords Autonomous Robot, Swarm Robotics, Collective Behaviour, Micro-robot

1. Introduction

Autonomous robot swarms [1] represent a fascinating, bio-inspired concept which provides a robust and flexible robotics system by exploiting large numbers of robots. This concept allows for the coordination of simple physical robots in order to cooperatively perform tasks. The decentralized control of robotic swarms can be achieved by providing well-defined interaction rules for each individual robot. These rules are executed continuously in an infinite loop and can provide for suitable collective behaviours in robotic environments [2]. Biological self-organization behaviours provide some of the best examples in setting up a robotic swarm system [3]. The collective behaviour in a group of robots emerges from interactions between simple agents, and so has an indirect relationship with the behaviour of each individual robot. A simple modification of an individual robot's behaviour could result in a significant change in the collective behaviour of the swarm. Therefore, the homogeneity of the robot platform is an important issue in executing robotic swarm scenarios. The platform must be able to imitate swarm behaviours found in nature, such as insects, birds and fish. It should be designed with compact physical dimensions to allow for the study of large-scale swarm behaviour in the lab area. A practical mechatronics design is required to simplify replication and ensure platform homogeneity, as in the standard definition of a robotic swarm system [4].

Robot	Cost	Sensor	Motion/Speed	Size	Autonomy
Colias	£25	distance, light, bump, bearing, range	wheel, 35 cm/s	4 cm	1-3 h
AMiR [5]	£65	distance, light, bearing	wheel, 10 cm/s	6.5 cm	2 h
Alice [6]	N/A	distance, camera	wheel, 4 cm/s	2.2	10 h
Jasmine [7]	£80	distance, light, bearing	wheel , N/A	3 cm	1-2 h
E-puck [8]	£580	distance, camera, bearing, accele, mic	wheel, 13 cm/s	7.5 cm	1-10 h
Kobot [9]	£800	distance, bearing, vision, compass	wheel , N/A	12 cm	10 h
Kilobot [10]	£75	distance, light	vibration, 1 cm/s	3.3 cm	3-24 h
R-one [11]	£220	light, IR, gyro, bump, accelerometer	wheel, 30 cm/s	10 cm	6 h
SwarmBot [12]	N/A	range, bearing, camera, bump	wheel, 50 cm/s	12.7 cm	3 h

Table 1. Comparison of some swarm robotics platforms

Several mobile robot platforms have previously been developed in studying swarm applications - these are shown in Table 1. *Alice* [6] is one such swarm robot built with a very small package size; it has been employed in various swarm research applications, such as the embodiment of cockroach aggregation [13]. The latest version of Alice is equipped with proximity sensors and infrared (IR) remote receivers. It can communicate with its direct neighbour using the IR sensors at short distances. The commercialized Alice was previously around a few hundred pounds. Another micro-robot which has been widely used in swarm robotics is *Jasmine* [7]. This robot uses six IR sensors to detect obstacles as well as robots in close proximity. Jasmine has played the role of a honeybee in several aggregation (BEECLUST) scenarios [14, 15]. *E-puck* [8] is one of the most successful robots, being mainly designed for education in the engineering field, and it is equipped with several sensors. However, the commercialized version of the basic e-puck is about £580 and an extra £300 is needed to obtain an additional range and bearing module [16]. *Kilobot* [10] is also a robot swarm platform with scalable functions, such as a group charger and programmer. It uses a slip-stick principle for motion which reduces its cost, since the robot does not use motors or wheels. However, the motion method has several drawbacks, such as that the achieved speed is low, which limits its application in swarm scenarios. Its method of motion reduces its use on various surfaces. We previously developed *AMiR* (Autonomous Miniature Robot) [5] as a low-cost open-hardware platform for swarm applications. It uses IR sensors for distance estimation and short-range communication. Several research applications have been performed with AMiR, including BEECLUST aggregation [17] and the extended version of BEECLUST [18–20]. Moreover, AMiR is simulated in Player/Stage and was used as the simulated robot swarm platform in [21]. Although the feasibility of AMiR for use in swarm robotics has been demonstrated, its motion is relatively slow and its size does not allow for the use of a large number of robots in a small arena. The limited range of communication is another disadvantage of AMiR which limits the scenarios to short-range coherent behaviours.

The simulation of large numbers of such robots is extremely complex and the results often do not meet the observed results of what would be exhibited in real robot experiments. Therefore, to imitate the bio-inspired mechanisms of swarm robots and to enable all research groups even with limited funding to perform such research with real robots, the robot platform must have the following criteria: low-cost design, long-term autonomy, long-range communication, bearing, distance and obstacle detection, neighbouring robot detection, fast motion, a small size and an open-source design.

We have developed a new platform to meet these requirements. The design of Colias was considered in terms of these requirements and, due to its small size and fast motion, experiments could be conducted both cost- and time-effectively in a small working area. In comparison to the other mobile robots which are utilized in swarm robotic research, Colias is a low-cost platform (about £25) and hence it is feasible for the easy and economic replication of large numbers of robots.

The rest of this paper is organized as follows. In Section 2, we introduce the hardware of the robot. Following that, in Section 3, we explain a swarm algorithm implemented by Colias. In Section 4, we discuss the experimental results of individual and social experiments. Finally, in Section 5, we draw conclusions and discuss the future research directions in which the robot might be involved.

2. Colias Design

In this section, we explain the designed hardware and control mechanism of Colias with regard to individual and social behaviours. Figure 1 shows a Colias robot and its different modules. The robot has two boards – upper and lower – which have different functions. The upper board is for high-level tasks, such as inter-robot communication and user-programmed scenarios; however, the lower board is designed for low-level functions such as power management and motion control.
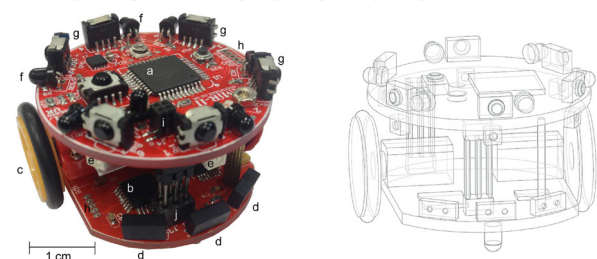
Figure 1. (Left) Colias mobile robot. a: Upper board processor, b: 2nd processor for motion and power management, c: 2.2 cm diameter wheels, d: proximity (bump) sensors, e: IR transmitters, f: IR phototransistors, g: IR decoders, h: SPI port, i: RS-232, j: I^2C and parallel links. (Right) A 3D simulated robot to be used in simulation software.
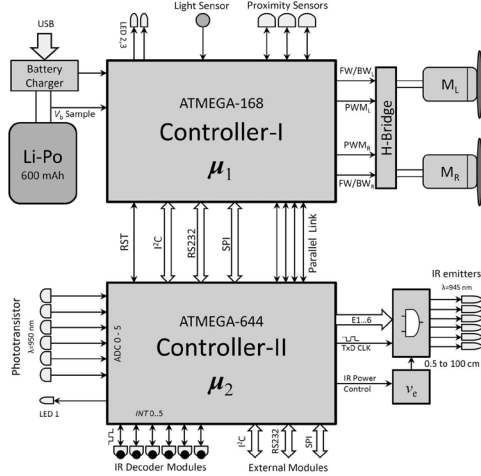
Figure 2. Basic architecture of Colias. The robot uses two processors in parallel which monitor all of its functions.

2.1. Controller

Colias employs two on-board ATMEL AVR micro-controllers in parallel: μ_1 and μ_2 (see Figure 2). The parallel processing provides for the fast and reliable control of different functions of the robot. As shown in the robot's basic architecture in Figure 2, the functions: i) power management, ii) obstacle detection and iii) motion control are managed by μ_1. Moreover, μ_2 controls the inter-robot communication and the user-programmed scenarios (individual and social tasks). The priority of the processors is programmable, although by default the high priority tasks are performed by μ_1.

Inter-processor communication is an important issue which affects the speed of processing and its reliability. Therefore, the robot employs two different links between its processors – parallel and serial. In the parallel link, both processors can be defined as a master or as a slave. With serial communication, the robot has three different links, namely, RS-232[1], I²C[2] and the SPI[3]. In general, all three serial links (buses) can be used to establish a connection between the processors. Moreover, these links are used to communicate with the external modules, such as the camera, the external memory and the robot-PC link. We also used the SPI bus to program the micro-controllers.

2.2. Motion

Two micro DC motors employing direct gears and two wheels with a diameter of 2.2 cm actuate Colias with a maximum speed of 35 cm/s. The rotational speed for each motor is controlled individually using a pulse-width modulation (PWM) technique [22]. Each motor is driven separately by a H-bridge DC motor driver and consumes

average power of 35±5 mA in no-load conditions and up to 150±20 mA in stall conditions. The robot uses the differential-driven configuration, which is a simple method to control a mobile robot using a very basic motion control principle. Since the motors are directly supplied by the battery of the robot, any changes in battery level will impact the speed of the robot. Therefore, we need to apply the battery level in the kinematic model.

The output voltage of the PWM (v_m) is a fraction of the maximum voltage of the source (E_{bat}) and duty cycle of the PWM signal (p); hence, $v_m = p \cdot E_{bat}$. We show the maximum velocity of the shaft spinning with a macroscopic model of the utilized motors [23]:

$$N_{max} = \alpha_m E_{bat} + \beta_m \quad , \qquad (1)$$

where α_m and β_m are two coefficients depending upon the motor's characteristics and the robot's design. Suitable values of α_m and β_m are extracted using empirical experiments.

The kinematic model of the robot follows general differential-driven kinematics:

$$\xi = \begin{bmatrix} x \\ y \\ \theta \end{bmatrix} = f(\varphi_l, \varphi_r, \delta t) \quad , \qquad (2)$$

which shows that the position estimation of the robot depends upon the speed of the left and right wheels ($\varphi_{l,r} = p_{l,r} N_{max} \pi d_w$) in a δt time span. p shows the duty cycle of the PWM for each wheel, which is a variable between 0 and 1.

As the employed motors' gearbox ratio is high (120:1) and the robot is lightweight (28 g), the robot does not need much torque ($\tau_m \cong 0$) to move. As a result, the acceleration of the motors is similar to the no-load condition and this causes the speed to settle within a few milliseconds. Since the dynamic analysis of the motion depends upon the acceleration, due to the elimination of the acceleration from the motion equations we do not need to model the dynamic motion of the robot.

2.3. Sensory System

The basic configuration of Colias uses only IR proximity sensors[4] to avoid obstacles as well as collisions with other robots, and a light sensor to read the illuminance of the ambient light. The IR sensory system consists of two different types of IR module, namely, short-range sensors (bump sensors, see Figure 1d) and long-range sensors (proximity sensors, see Figure 1 e and f). A combination of three short-range sensors and an independent processor grants the capacity for an individual process for obstacle detection which works in parallel with the rest of the system. A similar, although complex, mechanism has been

---

[1] Standard two-wire (RxD: Received Data and TxD: Transmitted Data) communication, also known as EIA-232. We used a TTL voltage level of 0 and 5 V).

[2] Inter-integrated Circuit, is a two-wire communication (SDA: Serial Data Line and SCL: Serial Clock) invented by Philips.

[3] Serial Peripheral Interface is a synchronous three-wire (MOSI: Master Output & Slave Input, MISO: Master Input & Slave Output and SCLK: Serial Clock generated by master) serial data link invented by Motorola. It is also used for micro-controllers programming.

[4] We used infrared emitters and receivers with a wavelength of 900nm< λ <980nm, to avoid any interference from the lighting system used in our laboratory environment.

found in locust vision, in which a specific neuron called the 'lobula giant movement detector' (LGMD) which reacts to objects approaching the insect's eyes [24].

The long-range system is composed of six IR proximity sensors (each 60° on the robot's upper board) for obstacle and robot detection [25]. The IR sensing system is able to distinguish robots from obstacles. The range of the system is approximately 15±1 cm with a radiant power of 6 mW/sr (adjustable up to 15 mW/sr).

Obstacle detection and distance estimation use the fundamental principles of electromagnetic radiation and its reflections. The reflected IR value that is measured by a sensor is mathematically modelled by the following equation [26]:

$$s(x, \theta) = \frac{\alpha_c \cos \theta}{x^2} + \beta_c \quad , \quad (3)$$

where $s(x, \theta)$ is the output value of the sensor, x is the distance of the obstacle, and θ is the angle of incidence with the surface. The model variable α_c includes several parameters, such as the reflectivity coefficient, the output power of the emitted IR and the sensitivity of the sensor. β_c is the offset value of the amplifier and ambient light effect. White body and black body surfaces reflect and absorb IR radiations with different ratios, which is a significant issue in selecting between obstacles and walls for robotic environments. The model parameters (α_c and β_c) are estimated empirically and are applied to future calculations.

In addition, the light sensor is placed at the bottom of the robot and is directly connected to both processors – μ_1 and μ_2. Therefore, each controller is able to translate the illuminance of the ambient light from an analogue value to a digital number between 0 and 255. In robot swarm scenarios, light is mostly used as a cue in the group-level task, such as with the aggregation of honeybees [14, 18].

Furthermore, the serial communication links (explained in the controller section) allow the robot to utilize an extra sensory system, such as camera or ultrasonic modules.

2.4. Inter-robot Communication

In multi-robot experiments, the robots need to utilize a communication media in order to share their information and make collective decisions. Wireless communication is generally used when a scenario is to be accomplished with mobile robots. In this regard, infrared is a suitable choice as an inter-robot communication medium for robotic swarm applications compared with other wireless communication techniques, such as radio frequency. The advantages of using IR in swarm applications include position estimation, neighbouring robot recognition and direct communication, and they can be utilized for obstacle avoidance [25].

Colias translates its IR receivers' values to estimate the distance and bearing of neighbouring robots. The distance of a neighbour can be simply judged by the amplitude of the received IR. Since the robot's receivers are placed apart symmetrically (60°), we can estimate the relative angular
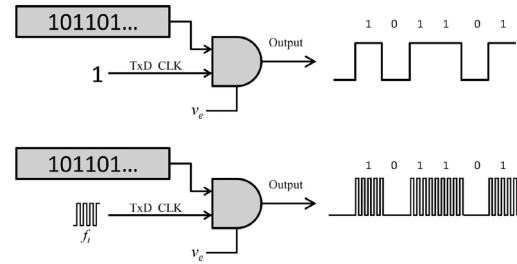
Figure 3. Amplitude-shift keying modulation for message transmission with (a) on/off and (b) pulse/off signals

position of the neighbouring robot using the following equation:

$$\phi = \operatorname{atan} \left(\frac{\sum_{i=1}^{6} \hat{s}_i \sin(\gamma_i)}{\sum_{i=1}^{6} \hat{s}_i \cos(\gamma_i)} \right) \quad , \quad (4)$$

where ϕ is the estimated angular position of the neighbour, γ_i is the angular distance between the ith sensor and the robot's head, and $\hat{s}_i, i \in \{1, 2, 3, 4, 5, 6\}$ is the translated IR intensity from sensor i.

The robot's message must be modulated and transmitted to its direct neighbours. There are several modulation techniques for data transmission. In general, two types of modulation methods are employed in short-range communication, which are: i) amplitude-shift keying (on/off mode), and ii) a mix of pulse and amplitude-shift keying. Figure 3 reveals the modulation methods which can be performed by Colias's communication module. As shown in the diagram, a TxD clock must be connected to a pulse generator with a frequency of f_t (for pulse/off modulation) or logic '1' (for on/off modulation). However, the TxD clock is fed by a timer of the main processor, and hence it does not need an external clock source. The frequency of modulation, f_t, depends upon the receivers' sampling rate. In our robot, we use a 38 kHz carrier frequency. Moreover, v_e adjusts the output power (amplitude) of the transmitter, which controls the maximum distance of communication.

Each message is formatted to 10 bits length, starting with a one bit preamble of logic '1'. The next eight bits are the actual message body [27]. The last bit is reserved for future communication methods between different robots in the case of heterogeneous scenarios. Since the communication messages are too short (10 bits), the robot uses a low data rate of 200 bps (20 messages/sec) for communication in order to increase the reliability of the communication and reduce the error rate.

2.5. Power Management

In swarm robot scenarios, the robot must have sufficient battery power to complete a given task. To achieve long-term autonomy, we need to have a proper power management system to monitor all the functions of the robot during a task and to control the battery charging current during a recharging process such that it increases the battery life. In Colias, the lower board is responsible for managing power consumption as well as the recharging process. The power consumption of the robot with normal

motion (in a quiet arena with only walls) and short-range communication (low-power IR emitter) is around 560 mA. However, it can be reduced to about 200 mA when the emitters are turned on only occasionally and the robot moves at a faster speed. A 3.7 V, 600 mAh (extendible up to 1200 mAh) lithium-polymer battery is used as the main power source, which gives autonomy of around three hours for the robot. More battery power is used by IR emitters and decoders when the emitter is turned on continuously. Therefore, the power consumption can be reduced to at least 50% by using pulse modulation in the IR emitters as well as a short data-packet size.

The recharging process of the battery is monitored by an external constant current/constant voltage linear charger IC (LTC4054-4.2). We fixed the charging current to a maximum of 400 mA in order to be able to use USB power to charge the battery.

Moreover, in-scenario recharging techniques, such as a docking charger [28–30] or movable chargers [31], can be applied to increase the autonomy time in long-term scenarios.

2.6. Firmware and Programming

In order to provide for simple programming and user-friendly robotic implementation, we provide various basic and high-level functions. The utilized swarm behaviours use sensors and received communication values to make a decision. Decisions are made in two different forms which are in programming routines, such as calling a function, and hardware modules, such as controlling motors or transmitting messages.

Microcontroller-based systems are flexible enough to use various programming languages and compilers. There are several types of compilers for AVR microcontrollers, such as assembly, C, Basic and Pascal. GNU [32] Compiler Collection (GCC) is a compiler of a GNU operating system that Colias uses for its programming.

3. Swarm Scenario

We evaluate the feasibility of Colias for use in collective swarm scenarios. In this regard, the state-of-the-art swarm aggregation algorithm (BEECLUST) [14] is implemented with different population sizes. Figure 4 reveals the behaviour of the each robot during the BEECLUST scenario. As can be seen in the diagram, the robots have a simple algorithm to follow. In general, after detecting an obstacle, a robot rotates and executes an obstacle avoidance routine. Alternatively, if the robot detects another robot, it stops and measures the illuminance of the ambient light. It is worth mentioning that a neighbour robot can be detected at a distance of 2 cm, which is called an 'inter-robot collision'. After each inter-robot collision, the robot waits. The duration spent waiting depends upon the measured illuminance. A higher light illuminance results in a longer stationary time. When the waiting time is over, the robot turns by a random degree and moves forward.
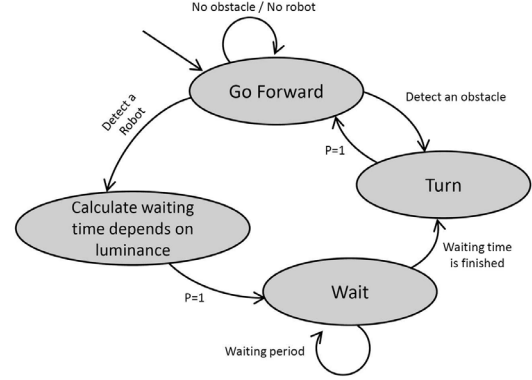
**Figure 4.** Finite state automaton that shows the robots' behaviour using BEECLUST

BEECLUST has been used in numerous swarm research applications as a bio-inspired aggregation algorithm with different configurations using real robots [7] and simulation software [33]. Mostly, gradient light is employed as the cue for the aggregation [14, 15, 18]. In addition, we previously implemented BEECLUST using a sound source as the cue for the aggregation [19, 20].
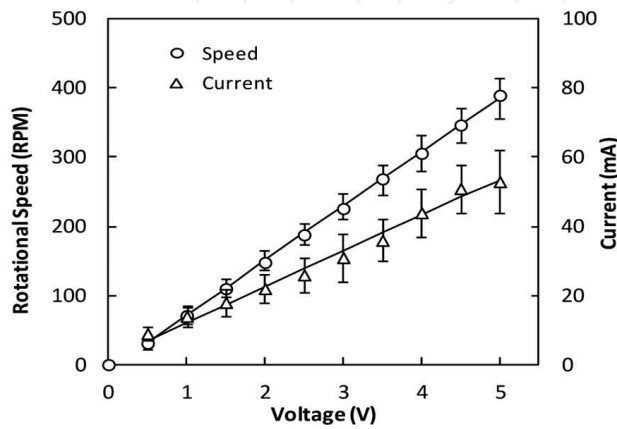
3.1. Arena Setup

To implement the scenario, we use a rectangular arena with a size of 95x55 cm. Two circular gradient light spots with a maximum illuminance of 420 lux are defined as the aggregation cues. Since the light sensor is placed at the bottom of the robot, we use a 42" LCD screen as the ground on which the robots move. The screen enables us to have a dynamic arena which is controlled by a computer. However, we need a small-sized and lightweight robot to implement the experiments on a LCD display. Figure 5 reveals the illuminance of the light in the defined aggregation zones. As can be seen in the light distribution in the arena, the maximum illuminance of the defined cues are slightly different. Therefore, there are two aggregation cues of differing luminance, which helps to test the discrimination ability of the aggregation method between two different sources. We tried to closely simulate the light spots on the screen as the real gradient of the light appears in the space. The aggregation zone is specified as two circular areas marked with drawn circles, as in Figure 11(a).
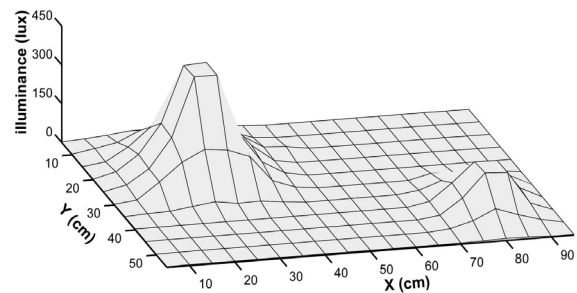
Figure 5. Sensory readings (illuminance of the light) of a robot placed at the indicated regions
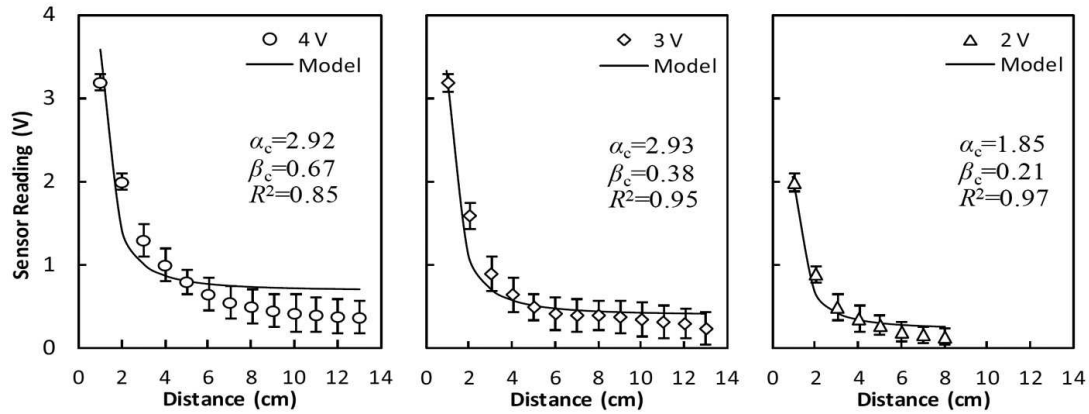
Figure 6. Median of sensor readings from 60 sensors for three power levels of the IR emitters ($v_e \in \{2, 3, 4\}$ V)

Figure 7. Median of the rotational speed and the motor's current as functions of the motor voltage

Figure 8. IR sensors reading (with Robot A) from the received IR emitted by a robot in front (Robot B in $0°$ orientation)
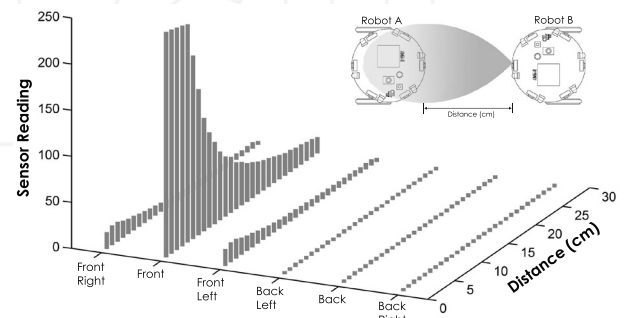
We use visual localization software developed by [34] to track the robots during the experiments using a mounted camera on top of the arena.

3.2. Metrics

In this work, two metrics are used: aggregation time and size of the aggregate. We defined two areas as the aggregation zones (zone A and zone B) and set the robots within those zones as the aggregated robots. The aggregation time, T_a, is defined as the time that the aggregate size reaches 70% of the total number of robots in zone A. The size of the aggregate, N_a, is the total number of robots within the aggregation zone A at a given time during the experiment.

4. Experiments and Results

The developed robot was evaluated during two different phases. During the first phase, we checked the functionality of the hardware of the mobile robot. Therefore, the actuator, sensory system and communication module of the robot were evaluated separately. During the second phase, we deployed Colias in a collective scenario, namely BEECLUST.

4.1. Modelling of Motion

To extract the model parameters (α_m and β_m) that are described by Eq. 1, we performed a set of experiments with 50 motors at different voltages. Figure 7 shows the median of the rotational speed and current of the motors for different voltages between 0.5 V and 5 V. The recorded results demonstrate a linear relationship between the rotational speed and the applied voltage. The proposed model with parameters of $\alpha_m = 78.45$ and $\beta_m = -6.50$ was perfectly fitted with a high coefficient of determination ($R^2 = 0.98$).

Moreover, the recorded current values from different applied voltages on the motors also displayed a linear increase by increasing the voltage.

4.2. Modelling of Proximity Sensors

As was mentioned in the hardware design section, Colias uses two types of IR sensors, namely: i) short-range proximity sensors (bump sensor) which detect an obstacle or a neighbour at a close distance of 3 ± 0.5 cm, and ii) medium-range sensors (IR proximity sensors) which can detect obstacles and other robots at greater distances. In this section, we present the results from the medium-range proximity sensors. Figure 6 illustrates the median of the captured sensors' readings from 10 robots (60 sensors) in different IR powers ($v_e \in \{2, 3, 4\}$ volts). The experiments were performed in a fluorescent lighted room. As shown
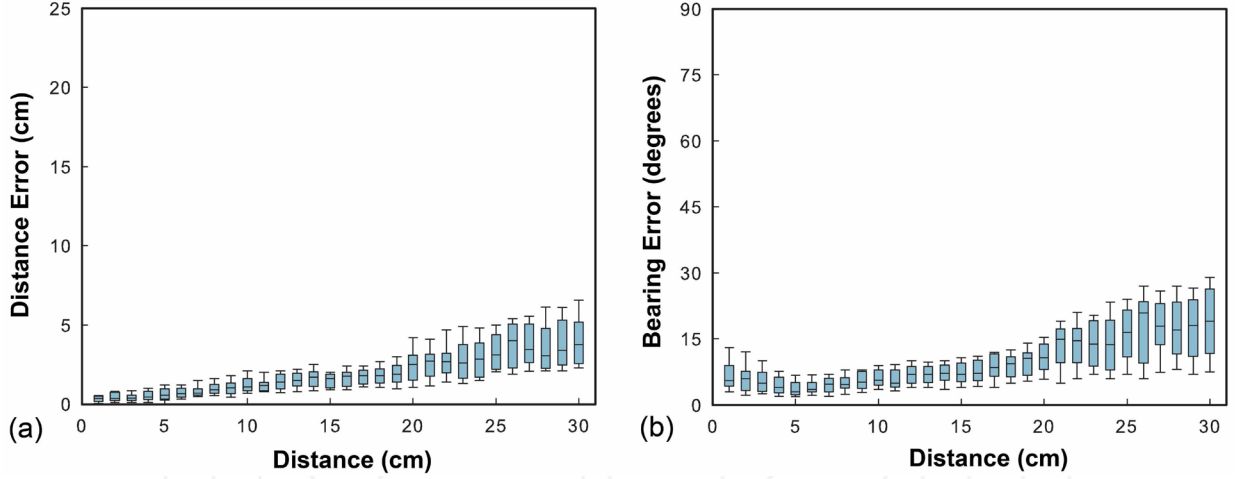
Figure 9. Error rates of distance estimation and bearing as functions of distance
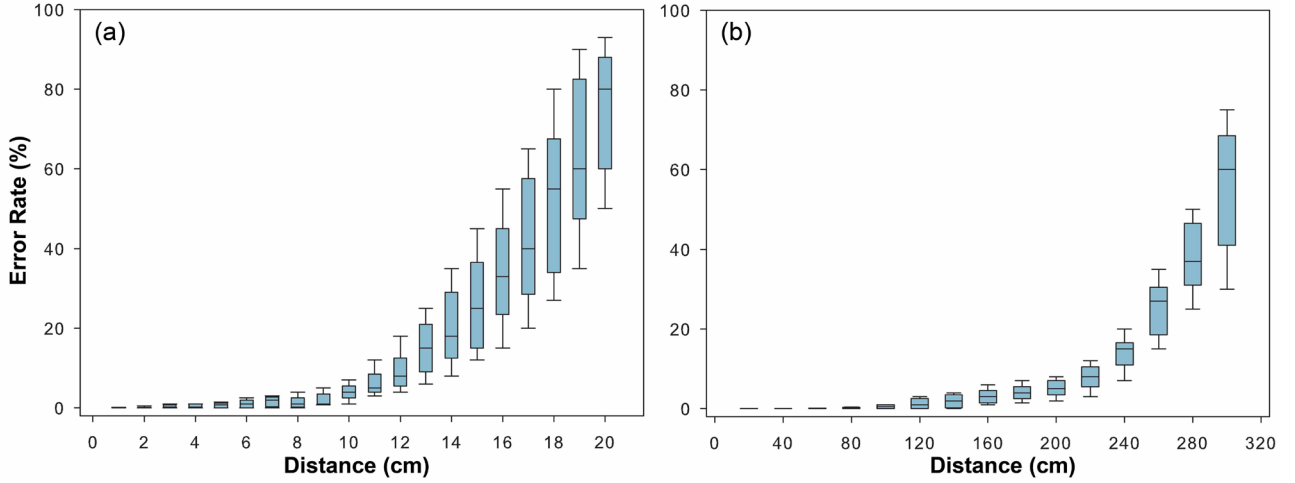
Figure 10. Inter-robot communication error rate of (a) short-range and (b) long-range communication
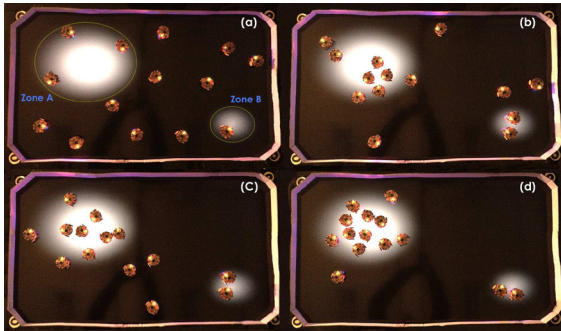

Figure 11. A sample run of the BEECLUST aggregation with 14 robots. Zone A is the aggregation zone with high illuminance (maximum illuminance of 420 lux) and Zone B is the low luminance source (maximum illuminance of 170 lux).

in the diagrams, the robot detects a white-body obstacle at long-range if the emitters' power is high. Therefore, with a maximum power of ($v_e = 4$ V), the robot detects a white-body obstacle at a distance of 10 ± 1 cm. However, at the minimum power level for the emitters, ($v_e = 2$ V), white-body obstacles can be detected at a distance of only 5 ± 1 cm.

The model parameters (Eq. 3) are approximated using the captured samples from the sensors at different distances. All the models are solved with high coefficients of determination (R^2). β_c reduces when the IR power decreases. α_c also shows the same behaviour, except at maximum power ($v_e = 4$V). At the high IR power, R^2 is also lower than the others. This is because of the sampling reference voltage of the ADC, which is fixed at 3.3 V. In other words, α_c and R^2 at $v_e = 4$ V would be higher values if the ADC's voltage references were set to a higher voltage than 4 V. However, with the Colias hardware, it is not possible to change the setting of the ADC voltage references. Although the model values at $v_e = 4$ V are not accurate, we can use the maximum power to detect obstacles at long distances.

In the case of robot-robot communication, we need to find the distance and relative orientation of any neighbouring robots. Figure 8 presents an example of the sensor readings for a neighbour robot (Robot-B) that is emitting IR in front of the receiver robot (Robot-A). As was expected, the direct sensor (*front*) receives higher amounts of IR than the neighbouring sensors (*front-right* and *front-left*).
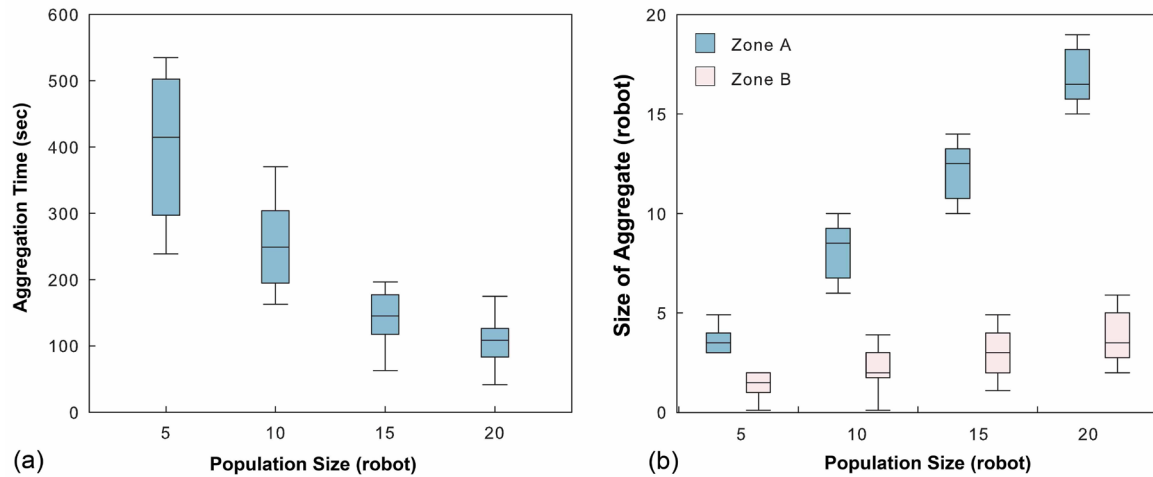
Figure 12. (a) Aggregation time as a function of population size ($N \in \{5, 10, 15, 20\}$). (b) Size of the aggregates in zones A and B for different population sizes.

This phenomenon allows us to model a bearing estimation using the existing sensors.

4.3. Inter-robot Communication

In another set of experiments, the robot receives IR from its neighbour at different distances and angles. The emitter robot uses $v_e = 3.3$ V and it is placed at different angles $\phi_n \in \{-60°, -30°, 0°, 30°, 60°\}$ and different distances ranging from 1 cm to 30 cm. The reading values are evaluated with the equations (3) and (4) and the error rates of the estimated distance and angle with respect to the real position and orientation of the robot, as illustrated in Figure 9. In the case of distance estimation, the model shows an average error rate of ± 1 cm up to 20 cm. The error rate increases significantly when increasing the distance up to 30 cm due to a reduction in IR strength. This is also seen with the bearing error rate such that where the error rate is $\pm 5°$ up to 20 cm, an increase in the distance results in a reduction of the accuracy of the bearing. However, at short distances (less than 3 cm), the bearing function shows a high error rate because of the transmitting angle of the emitter, which is $\pm 60°$; hence, at a short distance the emitted IR cannot reach the surrounding sensors and is only received by the direct one.

In addition, we tested the short-range and long-range inter-robot communications to calculate the packet error rates. We sent 1,000 packets (messages) and calculated the error rates in the receiver robots using 20 robots at $v_e = 3.3$ V. Figure 10 illustrates the error rates of the inter-robot communications at different distances. Two robots were faced towards one another, and hence their relative alignment was assumed to be $\theta = 0°$. In both cases, an increase in the distance between the robots reduces the performance of the communication due to a reduction in the IR signal strength. With the short-range communication, the robots exhibited relatively reliable communication at a distance of less than 12 cm. With the long-range communication, the robots could communicate up to 2 m with an acceptable error rate. Since the long-range module employs IR filters and an internal pulse

processing unit, the robot is able to communicate over a longer distance than the short-range module.

4.4. Swarm Scenario

The experiments in the swarm scenario (BEECLUST) were conducted with $N = \{5, 10, 15, 20\}$ robots. A sample run with Colias robots is shown in Figure 11 and the results are depicted in Figure 12. In general, when the swarm population increases, the aggregation becomes significantly faster (according to analysis of variance, P-value < 0.05), since an increase in the number of robots increases the probability of inter-robot collisions, which eventually causes a quicker aggregation. We also recorded the size of the aggregates in both zones A and B (Figure 12 b). The observed results show that the size of the aggregate in zone A increases significantly with increasing population size. However, the aggregation in zone B did not see a significant increase with an increase in the number of robots. Therefore, the discrimination ability of the aggregation method between two different sources is also demonstrated. The recorded results are dissimilar to the previous research on BEECLUST [7, 14, 18] due to the differing configuration of the experiments, such as the size of the arena and the robots deployed. In [7], the aggregation with 15 robots was accomplished in 65 sec; however, the experiment's configuration was different to our experiment. The Jasmine robots in that study moved at a speed of 30 cm/s using a sensing radius of 6 cm in an arena with area of 1.61 m². However, Colias moves at speed of 10 cm/s using a predefined perception range of 3 cm in an arena with an area of about 0.6 m². In comparison to [18] in which an aggregation with five robots was accomplished in 470 sec, AMiR is almost twice as large as Colias, with perception radius of 12 cm. It moves at the same speed in an arena with a size of about 1 m². Moreover, the BEECLUST aggregation using other types of cues [19, 20] showed various aggregation times compared to the recorded results in this section. Thus, BEECLUST aggregation relies significantly on the experiment's configuration.

Based on the observed results of the performed experiments regarding social and individual behaviours, the feasibility of the developed robot for use in swarm scenarios has been demonstrated. Since the robot is designed with a small package size, it would be possible to use large numbers of the robots in real robot scenarios.

5. Conclusion

The development of a new, low-cost (about £25), open-hardware platform was presented. The preliminary experiments were performed on hardware components such as actuators and sensory systems. We modelled the motion and sensory system of the robot mathematically and the model parameters were extracted empirically. Therefore, the feasibility of the developed robot as an autonomous platform has been demonstrated. Since Colias is developed for use in swarm robotics research, it played a honeybee role in a bio-inspired scenario called 'honeybee aggregation'. The results showed that the robot is highly amenable to deployment in collective behaviours. Although the robot has a basic sensory system and supports inter-robot communication, for some complex scenarios which require higher levels of perception we decided to add new features to the robot. For our future work, we are working on an extension of the vision module with a fast ARM processor to implement bio-inspired vision mechanisms.

6. Acknowledgement

7. References

[1] M. Brambilla, E. Ferrante, M. Birattari, and M. Dorigo. Swarm robotics: a review from the swarm engineering perspective. *Swarm Intelligence*, 7(1):1–41, 2013.

[2] D. D. Dudenhoeffer and M. P. Jones. A formation behavior for large-scale micro-robot force deployment. In *Simulation Conference Proceedings*, volume 1, pages 972–982, 2000.

[3] S. Camazine, N.R. Franks, J. Sneyd, E. Bonabeau, J.-L. Deneubourg, and G. Theraulaz. *Self-organization in biological systems*. Princeton University Press, 2003.

[4] E. Şahin. Swarm robotics: From sources of inspiration to domains of application. In *Lecture Notes in Computer Science*, volume 3342, pages 10–20. Springer, 2005.

[5] F. Arvin, K. Samsudin, and A. R. Ramli. Development of a Miniature Robot for Swarm Robotic Application. *International Journal of Computer and Electrical Engineering*, 1:436–442, 2009.

[6] G. Caprari, T. Estier, and R. Siegwart. Fascination of down scaling - alice the sugar cube robot. *Journal of Micro-Mechatronics*, 1(3):177–189, 2002.

[7] S. Kernbach, R. Thenius, O. Kernbach, and T. Schmickl. Re-embodiment of Honeybee Aggregation Behavior in an Artificial Micro-Robotic System. *Adaptive Behavior*, 17(3):237–259, 2009.

[8] F. Mondada, M. Bonani, X. Raemy, J. Pugh, C. Cianci, A. Klaptocz, S. Magnenat, J-C. Zufferey, D. Floreano, and A. Martinoli. The e-puck, a robot designed for education in engineering. In *Proceedings of the 9th conference on autonomous robot systems and competitions*, volume 1, pages 59–65, 2009.

[9] A. E. Turgut, H. Çelikkanat, F. Gökçe, and E. Şahin. Self-organized Flocking in Mobile Robot Swarms. *Swarm Intelligence*, 2(2):97–120, 2008.

[10] M. Rubenstein, C. Ahler, and R. Nagpal. Kilobot: A low cost scalable robot system for collective behaviors. In *IEEE International Conference on Robotics and Automation*, pages 3293–3298, 2012.

[11] J. McLurkin, A. J. Lynch, S. Rixner, T.W. Barr, A. Chou, K. Foster, and S. Bilstein. A Low-Cost Multi-robot System for Research, Teaching, and Outreach. In *Distributed Autonomous Robotic Systems*, volume 83, pages 597–609, 2013.

[12] J. McLurkin, J. Smith, J. Frankel, D. Sotkowitz, D. Blau, and B. Schmidt. Speaking swarmish: Human-robot interface design for large swarms of autonomous mobile robots. In *AAAI spring symposium*, 2006.

[13] S. Garnier, C. Jost, J. Gautrais, M. Asadpour, G. Caprari, R. Jeanson, A. Grimal, and G. Theraulaz. The embodiment of cockroach aggregation behavior in a group of micro-robots. *Artificial Life*, 14(4):387–408, 2008.

[14] T. Schmickl, R. Thenius, C. Moeslinger, G. Radspieler, S. Kernbach, M. Szymanski, and K. Crailsheim. Get in touch: cooperative decision making based on robot-to-robot collisions. *Autonomous Agents and Multi-Agent Systems*, 18(1):133–155, 2009.

[15] M. Bodi, R. Thenius, M. Szopek, T. Schmickl, and K. Crailsheim. Interaction of robot swarms using the honeybee-inspired control algorithm BEECLUST. *Mathematical and Computer Modelling of Dynamical Systems*, 18(1):87–100, 2012.

[16] A. Gutiérrez, A. Campo, M. Dorigo, D. Amor, L. Magdalena, and F. Monasterio-Huelin. An open localization and local communication embodied sensor. *Sensors*, 8(11):7545–7563, 2008.

[17] F. Arvin, S. Doraisamy, K. Samsudin, F. A. Ahmad, and A. R. Ramli. Implementation of a Cue-Based Aggregation with a Swarm Robotic System. In *Communications in Computer and Information Science*, volume 295, pages 113–122. Springer, 2012.

[18] F. Arvin, K. Samsudin, A. R. Ramli, and M. Bekravi. Imitation of Honeybee Aggregation with Collective Behavior of Swarm Robots. *International Journal of Computational Intelligence Systems*, 4(4):739–748, 2011.

[19] F. Arvin, A. E. Turgut, and S. Yue. Fuzzy-Based Aggregation with a Mobile Robot Swarm. In *Swarm Intelligence*, volume 7461 of *Lecture Notes in Computer Science*, pages 346–347. Springer, 2012.

[20] F. Arvin, A. E. Turgut, F. Bazyari, K. B. Arikan, N. Bellotto, and S. Yue. Cue-based aggregation with a mobile robot swarm: a novel fuzzy-based method. *Adaptive Behavior*, 22(3):189–206, 2014.

[21] F. A. Ahmad, A.R. Ramli, K. Samsudin, and S. J. Hashim. Energy management in mobile robotics system based on biologically inspired honeybees behavior. In *IEEE International Conference on Computer Applications and Industrial Electronics*, pages 32–35, 2011.

[22] F. Arvin, K. Samsudin, and M. A. Nasseri. Design of Differential-Drive Wheeled Robot Controller with Pulse-Width Modulation. In *IEEE Conference on Innovative Technologies in Intelligent Systems and Industrial Applications*, pages 143–147, 2009.

[23] F. Arvin and M. Bekravi. Encoderless position estimation and error correction techniques for miniature mobile robots. *Turkish Journal of Electrical Engineering & Computer Sciences*, 21:1631–1645, 2013.

[24] S. Yue, F. C. Rind, M. S. Keil, J. Cuadri, and R. Stafford. A bio-inspired visual collision detection mechanism for cars: Optimisation of a model of a locust neuron to a novel environment. *Neurocomputing*, 69:1591 – 1598, 2006.

[25] F. Arvin, K. Samsudin, and A. R. Ramli. Development of IR-Based Short-Range Communication Techniques for Swarm Robot Applications. *Advances in Electrical and Computer Engineering*, 10(4):61–68, 2010.

[26] G. Benet, F. Blanes, J. E Simó, and P. Pérez. Using infrared sensors for distance measurement in mobile robots. *Robotics and autonomous systems*, 40(4):255–266, 2002.

[27] F. Arvin, K. Samsudin, and A. R. Ramli. A short-range infrared communication for swarm mobile robots. In *International Conference on Signal Processing Systems*, pages 454–458. IEEE, 2009.

[28] M. C. Silverman, D. Nies, B. Jung, and G. S. Sukhatme. Staying alive: A docking station for autonomous robot recharging. In *IEEE International Conference on Robotics and Automation*, volume 1, pages 1050–1055, 2002.

[29] A. Attarzadeh. Development of advanced power management for autonomous micro-robots. Master's thesis, University of Stuttgart, Germany, 2006.

[30] F. Vaussard, P. Rétornaz, S. Roelofsen, M. Bonani, F. Rey, and F. Mondada. Towards long-term collective experiments. In *Intelligent Autonomous Systems*, volume 194 of *Advances in Intelligent Systems and Computing*, pages 683–692. 2013.

[31] F. Arvin, K. Samsudin, and A.R. Ramli. Swarm Robots Long Term Autonomy Using Moveable Charger. In *International Conference on Future Computer and Communication*, pages 127 – 130, 2009.

[32] R.M. Stallman. The GNU project, 1999.

[33] D. Kengyel, R. Thenius, K. Crailsheim, and T. Schmick. Influence of a Social Gradient on a Swarm of Agents Controlled by the BEECLUST Algorithm. In *European Conference on Artificial Life*, pages 1041–1048, 2013.

[34] T. Krajník, M. Nitsche, J. Faigl, T. Duckett, M. Mejail, and L. Přeučil. External Localization System for Mobile Robotics. In *Proceedings of the International Conference on Advanced Robotics*, 2013.